Miniaturized and Reconfigurable Rat-Race Coupler Based on Artificial Transmission Lines

Miniaturized and Reconfigurable Rat-Race Coupler based on Artificial Transmission Lines

E. Tolin, A. Bahr, and F. Vipiana, *Senior Member, IEEE*

***Abstract*— A miniaturized and reconfigurable rat-race coupler realized in inexpensive PCB technology is proposed. Miniaturization is achieved by exploiting the theory of right- and left-handed artificial transmission lines. The frequency agility allows the rat-race coupler to operate at two bands centered at 900 MHz and 1.7 GHz, therefore covering many industrial and communication standards. The frequency selection is operated by CMOS switches, controlled by only 1-bit signal, for adapting the equivalent electrical length of the four branches of the coupler. Moreover, the dimension is significantly reduced with respect to standard realizations at the same frequencies, with required areas of about 3% at 900 MHz and 10.4% at 1.7 GHz. The proposed design has been fabricated and measured, showing good performance in both operative frequency bands.**

***Index Terms*— Artificial transmission lines, coupler, reconfigurable.**

I. Introduction

With the increase of multifunctional devices and integration of several wireless standards in a single system, nowadays much research is focused on multi-band and miniaturized components. In this context, the rat-race coupler is a fundamental element for many circuits and applications, offering the unique possibility to be used as in-phase or out-of-phase combiner. However, this coupler also exhibits well-known drawbacks, such as its large area and narrow bandwidth [1]. For these reasons, several studies have been focused on the size reduction, employing techniques such as slow wave structures, metamaterials and folding technology (see e.g. [2] – [6]). Moreover, another important topic is represented by the design of multi-band and dual-mode rat-race couplers [7], [8]. However, limited effort was spent to introduce frequency reconfigurability [9], [10].

The goal of this letter is to realize a compact rat-race coupler with reconfigurable operation over 900 MHz and 1.7 GHz, thus including important industrial (e.g. RFID), satellite (e.g. GPS, Iridium) and mobile communication standards (e.g. GSM 900 and 1800 in both uplink and downlink).

Manuscript received XXXX 20XX.

E. Tolin and F. Vipiana are with the Department of Electronics and Telecommunications, Politecnico di Torino, Italy (email: {enrico.tolin, francesca.vipiana}@polito.it).

A. Bahr is with the Department of Antenna and EM Modelling, IMST GmbH, Kamp-Lintfort, Germany (email: achim.bahr@imst.com).

Color versions of one or more of the figures in his paper are available online at http://ieeexploire.ieee.org.

Digital Object Identifier xxxxxxxyyyyyyyzzzzzz.

II. Rat-race Coupler Design

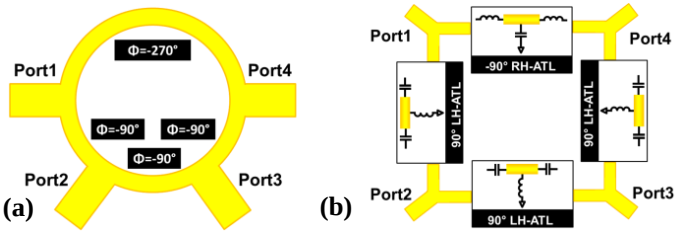

Fig. 1. Scheme of the (a) standard and (b) proposed rat-race design.

Slow wave structures are an essential methodology for achieving miniaturization [11]. As depicted in Fig. 1, where a comparison between the proposed and the standard design is shown, the slow wave technique is used for designing the four branches of the rat-race coupler via artificial transmission line, by exploiting the dual periodic structures that synthesize right- and left-handed artificial transmission lines, indicated in the following as RH- and LH-ATLs respectively [12]-[13]. Both ATLs have the unique feature of realizing lines with almost arbitrary electrical length, independently from the physical dimensions, based on the cascade of many unit cells. Hence, the total phase incurred (positive for LH-ATLs, negative for RH-ATLs) is controlled by the contribution of a single unit cell and its aggregate. Therefore, as shown in Fig. 1.(b), here we propose to synthesize the +90° branches of the rat-race coupler by means of LH-ATLs, and, by exploiting the duality between the phase contributions of RH- and LH-ATLs (opposite in sign), -90° RH-ATLs is used instead of the long 270° branch. Hence, this solution avoids the use of a high number of unit cells that would increase losses and reduces the bandwidth. The symmetric T-shaped unit cell is used as circuital model for both ATLs, which is composed by a microstrip loaded with series impedance Z and shunt admittance Y (respectively equal to capacitor "C" and inductor "L" for LH-ATLs, while for RH-ATLs the definition is dual). The values of Z and Y are found from the dispersion relation of the periodic structure as described in [11] and [12]:

$$cos\varphi_x^* = \left(1 + \frac{Z\,Y}{4}\right) cos\theta_x + \frac{j}{2}\left(\frac{Z}{Z_B} + Y\,Z_B\right) sin\theta_x + \frac{Z\,Y}{4} \quad (1)$$

where θ_x and φ_x^* are the phases of the microstrip line and one unit cell respectively (with $x = 1$ or 2, according to the chosen frequency f_1 or f_2, assuming $f_2 > f_1$), and Z_B is the Bloch impedance. Furthermore, we note that the relation $L = C\,Z_B^2$ is used in the evaluation of the two unknowns Z and Y in (1). According to theory, Z_B is set equal to the characteristic

impedance of the rat-race branches, namely $\sqrt{2}\,Z_o$ (being $Z_o = 50\,\Omega$). Moreover, in the proposed design, the combination of LH/RH lines is also used as basis for applying frequency agility. The key principle consists of inserting (or removing) unit cells for attaining the desired electrical length at the specific design frequency. The proposed method allows to theoretically synthesize a multi-band rat-race with arbitrary frequency ratio. In this letter, reconfigurability is operated by using transfer and differential switches that allow a compact design, requiring only 1-bit control to change between the two bands. However, these kinds of switches are intended for 50 Ω applications only, thus introducing an impedance discontinuity in the rat-race branches. For this reason, in our realization we limit the maximum working frequency at around 2 GHz, where the impedance discontinuity is acceptable.

A. +90° Artificial Transmission Line Design

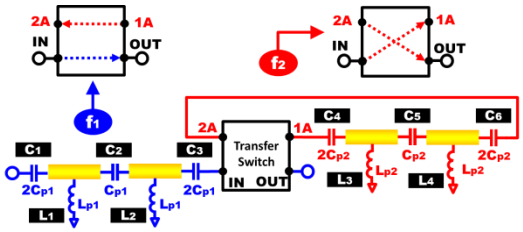

Fig. 2. Configurations of the +90° frequency agile branch at f_1 and f_2.

In Fig. 2 the principle of operation of the reconfigurable +90° branch based on LH-ATLs is shown, where only two unit cells are used ($n = 2$), for enhancing miniaturization. For the precise definition of the unit cell, we have to consider the phase contribution of all components, including the switch, that is expressed by the length l_s and phase constant $\beta_s(f_x)$. Similarly, θ_x in (1) will be expressed in terms of length l_l and phase constant $\beta_l(f_x)$. At first, the configuration for attaining the +90° state at f_1 is considered. The required phase per LH-ATL unit cell $\varphi_1^+(f_1)$, defined by (2), is found by adding all phase contributions of the bottom left components in Fig. 2:

$$\varphi_1^+(f_1) = \frac{1}{\omega_1\sqrt{L_{p1}C_{p1}}} - \beta_l(f_1)\,l_l \tag{2}$$

$$n\,\varphi_1^+(f_1) - \beta_s(f_1)\,l_s = \frac{\pi}{2} \tag{3}$$

where ω_1 is the angular frequency $2\pi f_1$. Therefore, $\varphi_1^+(f_1)$ is derived from (3) and, then, the values of components C_{p1} and L_{p1} in (2) are evaluated using (1).

The frequency agility is achieved by adding LH-ATL unit cells ($m_1 = 2$), for attaining the +90° phase value at frequency f_2, while maintaining unchanged the remaining part of the design. Hence, the total phase equation is written by considering all contributions depicted in Fig. 2:

$$\varphi_2^+(f_2) = \frac{1}{\omega_2\sqrt{L_{p2}C_{p2}}} - \beta_l(f_2)\,l_l \tag{4}$$

$$m_1\,\varphi_2^+(f_2) - 2\,\beta_s(f_2)\,l_s + n\varphi_1^+(f_2) = \frac{\pi}{2} \tag{5}$$

where $\varphi_2^+(f_2)$ is the phase per unit cell of the added section. In this case the delay caused by the transfer switch operating in crossing mode is multiplied by two. Lastly, L_{p2} and C_{p2} in (4) are computed using (5) via (1) as described before.

B. -90° Artificial Transmission Line Design

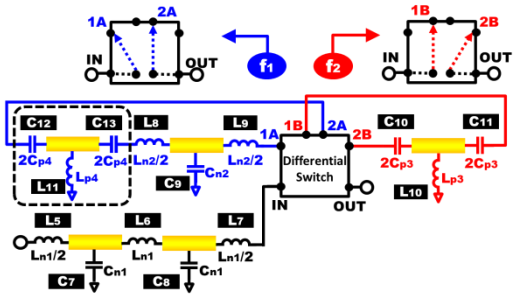

Fig. 3. Configurations of the -90° frequency agile branch at f_1 and f_2.

A different procedure is applied for the design of the -90° branch that replaces the long 270° section of the coupler. By using the RH-ATLs, more cells are needed to achieve -90° at f_1 and, for this reason, the f_2 operation is considered first. Moreover, for ensuring a wide band behavior, the derivative with respect to the angular frequency $\omega_2 = 2\pi f_2$ of the total phase condition for the -90° branch, defined in (8), has to be as close as possible to the one given by the +90° branch, expressed by (5). This is equivalent to set the same group delay at the center frequency. Since for RH-ATL the group delay is constant with respect to ω_2, we have to use the LH-ATL as Phase Balancing Term (PBT), thus achieving the same group delay characteristic over frequency of (5), which is squared (i.e. $\sim 1/\omega^2$). Then, $\varphi_2^-(f_2)$ in (6) and $\varphi_2^C(f_2)$ in (7) express the phase per unit cell of the RH-ATL and the PBT respectively, while (8) specify the phase condition for the -90° branch at f_2, with $n = 2$ and $m_2 = 1$, as illustrated in Fig. 3:

$$\varphi_2^-(f_2) = -\left[\beta_l(f_2)\,l_l + \sqrt{L_{n1}C_{n1}}\right] \tag{6}$$

$$\varphi_2^C(f_2) = \frac{1}{\omega_2\sqrt{L_{p3}C_{p3}}} - \beta_l(f_2)\,l_l \tag{7}$$

$$n\,\varphi_2^-(f_2) - 2\,\beta_s(f_2)\,l_s + m_2\,\varphi_2^C(f_2) = -\frac{\pi}{2} \tag{8}$$

$$\varphi_2^C(f_2) = \frac{1}{m_2}\left[2\,\beta_s(f_2)\,l_s + (m_1 + n - m_2)\,\beta_l(f_2)\,l_l\right] \tag{9}$$

Then, the PBT term is evaluated by imposing the condition on the +90° and -90° branch group delay equality at f_2, obtaining (9). Thus, by substituting (9) into (8), the phase per unit cell $\varphi_2^-(f_2)$ is derived, and then, as in the previous cases, L_{n1} and C_{n1} are computed via (1). Similarly, the values of C_{p3} and L_{p3} are calculated via (1) from the value of the phase found in (9).

In order to reach the -90° condition at f_1, more RH-ATL unit cells have to be added, as done for the design of the +90° branch at f_2 in Sect II.A. Therefore, the required phase for the -90° branch $\varphi_1^-(f_1)$ and the $\varphi_1^C(f_1)$ PBT at f_1 are expressed by (10) and (11) respectively. By following the same procedure described for the design of the -90° branch at f_2, (13) is derived from the phase derivative equality, while (12) sums all phase contributions and imposes the phase condition:

$$\varphi_1^-(f_1) = -\left[\beta_l(f_1)\,l_l + \omega_1\sqrt{L_{n2}C_{n2}}\right] \tag{10}$$

$$\varphi_1^C(f_1) = \frac{1}{\omega_1\sqrt{L_{p4}C_{p4}}} - \beta_l(f_1)\,l_l \tag{11}$$

$$-n\varphi_2^-(f_1) - 2\beta_s(f_1)\,l_s + m_3\varphi_1^-(f_1) + m_4\varphi_1^C(f_1) = -\frac{\pi}{2} \tag{12}$$

$$\varphi_1^C(f_1) = \frac{1}{m_4}\left[\beta_s(f_2)\,l_s + (n - m_4)\,\beta_l(f_1)\,l_l\right] \tag{13}$$

with $m_3 = 1$ and $m_4 = 1$ number of unit cells of the added RH-ATL and PBT sections respectively. Finally, the values of C_{p4}, L_{p4} and L_{n2}, C_{n2} are computed via (1) from the unit cell contribution found in (10) and (11) by plugging (13) into (12).

III. Realization and Experimental Results

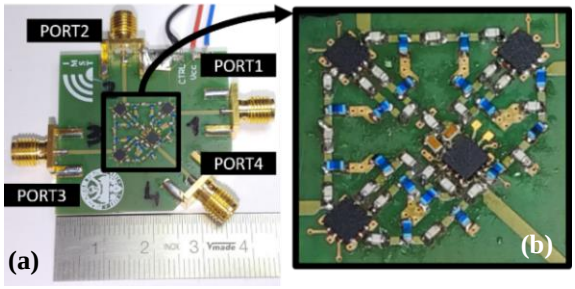

Fig. 4. (a): manufactured and assembled reconfigurable rat-race coupler; (b): enlargement of the RH-ATL and LH-ATL based branches with switches.

TABLE I
Values Of Components Loading The LH-ATL And RH-ATL Lines

Frequency	90° Branch	-90° Branch	
900MHz	C_1= C_3=4.7pF, C_2=2.5pF L_1= L_2=13nH	L_5=L_7=2.7nH C_7=C_8=1 pF L_6= 5.6nH	L_8=L_9=1nH C_9 =0.3pF
1.7GHz	C_4=C_6=2.5pF, C_5=1.2pF L_3=L_4 =6.8nH		C_{10}=C_{11}=2.3pF L_{10} =5.1nH

Fig. 4 shows the detail of the manufactured and measured compact frequency-agile rat-race coupler for the frequencies $f_1 = 900$ MHz and $f_2 = 1.7$ GHz. Inexpensive 0.5 mm thick FR4 substrate, characterized by $\varepsilon_r = 4.4$ and $\tan\delta = 0.02$, has been used. The section of microstrip line has length $l_l = 2.5$ mm, while the phase incurred by the switches have been found from measurements to be equivalent to a 50 Ω line with length $l_s = 5.6$ mm. Moreover, three QPC6222 [14] transfer switches and one RFSW6232 [15] differential switch from QORVO have been employed. In the final realization the phase balancing terms in the -90° branch at f_1 (enclosed by dashed line in Fig. 3) was omitted, because its contribution was found to be negligible. Referring to the notation reported in Fig. 2 and Fig. 3, Table I displays the used values, selected among the muRata series GJM15 for capacitors and LQW15/LQP15 for inductors. The theoretical values calculated as described in Sect. II have been optimized by employing the muRata library in ADS. The final selection of components was adjusted through measurements, for accounting for the real behavior of components. Fig. 5.(a)-(b) shows the good agreement between simulated and measured S-parameters of the rat-race coupler, evaluated in out-of-phase operation (Port1 excited) in the 900 MHz and 1.7 GHz bands respectively. The higher insertion loss, compared to non-reconfigurable couplers, is mostly due to the loss of the switches, which has to be counted twice in some configurations. We notice that the major effect on the phase imbalance, shown in Fig. 5.(c)-(d), is related to the LH-ATLs in the lower part of the bands (steepest variation of group delay), while, in the upper side of the bands, the dominant effect is given by the RH-ATLs. Furthermore, in Fig. 5.(c), a wideband behavior of the amplitude difference between $|S_{12}|$ and $|S_{14}|$ and phase imbalance $\angle S_{12} - \angle S_{14}$ are reported for the 900 MHz band. In Fig. 5.(d), we note that the bandwidth at 1.7 GHz is narrower than the 900 MHz case: this is mostly due to the effect of the switches, which are directly related to the phase contribution of the PBT, as revealed by (9) and (13). Moreover, from Fig. 5.(d), the flattening effect of the phase due to the PBT is evident, thus confirming the analysis carried in Sect II.B. We also observe that the choice of the 50 Ω switches do not compromise the overall performance. Finally, Table II summarizes the measured performance of the proposed rat-race coupler, including a comparison with other designs concerning miniaturization and frequency agility, developed in microstrip technology and in a similar frequency range. We note that the proposed realization at 900 MHz is the most compact at this frequency, to author's best knowledge.

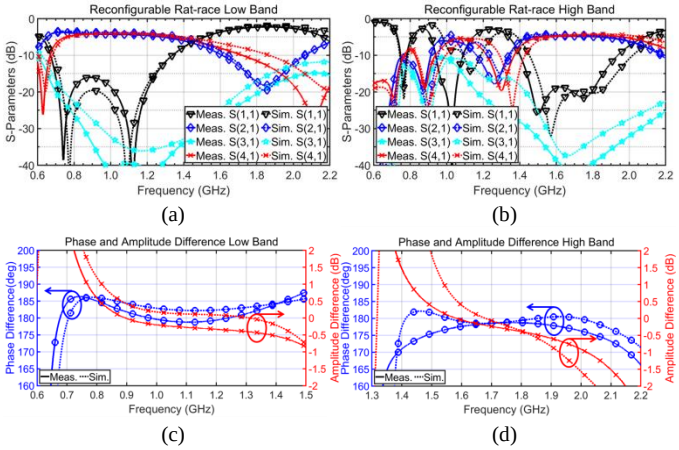

Fig. 5. Measured (solid line) and simulated (dashed line) S-parameters and phase/amplitude imbalance with Port1 excited: (a), (c) 900 MHz configuration and (b), (d) 1.7 GHz configuration.

TABLE II
Comparison Of Rat-Race Couplers Measured Performance

Ref.	Center Frequency	Band-Width*	Insertion Loss	Return Loss	Isolation	Relative Area**
[2]	900MHz	34%	3.5dB	10dB	9dB	3.9%
[5]	1.44GHz	10.5%	N/A	15dB	>20dB	8%
[6]	900MHz	57.5%	3.5dB	16dB	35dB	5.28%
[10]	0.84 - 2.48 GHz	50MHz	4.7 - 4.9 dB	15dB	20dB	15.92%
This work	900MHz	64%	3.9dB	10dB	26dB	3.03%
	1.7GHz	24%	4.3 dB	15dB	30dB	10.42%

(*) ±0.5dB amplitude variation and 10dB return loss criterion; in [10] the bandwidth is reported in MHz because the central freq. varies continuously.
(**) Compared to standard designs at same center frequency

IV. Conclusion and Perspectives

In this letter, a novel frequency agile rat-race coupler based on standard and inexpensive PCB technology has been designed and experimentally validated. By exploiting the LH-ATL and RH-ATL techniques, a conspicuous miniaturization is achieved. By reconfiguring the equivalent electrical length of the rat-race branches by adding/removing unit cells, two independent frequency operations are obtained, acting on a single control. Furthermore, the procedure describes a method for maintaining a broadband behavior of the device. As further perspective, a multiband rat-race coupler with three bands can be designed. Moreover, an improvement in cross-isolation among the two bands can be investigated. The same technique can be used also to design a 90° reconfigurable hybrid coupler.

REFERENCES

[1] H. Xu, G. Wang and K. Lu, "Microstrip Rat-Race Couplers," in *IEEE Microwave Magazine*, vol. 12, no. 4, pp. 117-129, June 2011.

[2] C. Tseng and H. Chen, "Compact Rat-Race Coupler Using Shunt-Stub-Based Artificial Transmission Lines," *IEEE Microwave and Wireless Components Letters*, vol. 18, no. 11, pp. 734-736, Nov. 2008.

[3] H. Okabe, C. Caloz and T. Itoh, "A compact enhanced-bandwidth hybrid ring using an artificial lumped-element left-handed transmission-line section," in *IEEE Transactions on Microwave Theory and Techniques*, vol. 52, no. 3, pp. 798-804, March 2004.

[4] H. Ghali and T. A. Moselhy, "Miniaturized fractal rat-race, branch-line, and coupled-line hybrids," in *IEEE Transactions on Microwave Theory and Techniques*, vol. 52, no. 11, pp. 2513-2520, Nov. 2004.

[5] J. Wang, B. -. Wang, Y. -. Guo, L. c. Ong and S. Xiao, "Compact slow-wave microstrip rat-race ring coupler," in *Electronics Letters*, vol. 43, no. 2, pp. 111-113, 18 January 2007.

[6] W. Chang, C. Liang and C. Chang, "Slow-Wave Broadside-Coupled Microstrip Lines and Its Application to the Rat-Race Coupler," *IEEE Microwave and Wireless Components Letters*, vol. 25, no. 6, pp. 361-363, June 2015.

[7] L. Cai and K. M. Cheng, "A Novel Design of Dual-Band Rat-Race Coupler With Reconfigurable Power-Dividing Ratio," *IEEE Microwave and Wireless Components Letters*, vol. 28, no. 1, pp. 16-18, Jan. 2018.

[8] L. Chang and T. Ma, "Dual-Mode Branch-Line/Rat-Race Coupler Using Composite Right-/Left-Handed Lines," *IEEE Microwave and Wireless Components Letters*, vol. 27, no. 5, pp. 449-451, May 2017.

[9] B. Dwivedy, S. K. Behera and D. Mishra, "Design of a frequency agile rat race coupler," *2015 IEEE Applied Electromagnetics Conference (AEMC)*, Guwahati, 2015, pp. 1-2.

[10] X. Tan and F. Lin, "A Novel Rat-Race Coupler with Widely Tunable Frequency," *IEEE Transactions on Microwave Theory and Techniques*, vol. 67, no. 3, pp. 957-967, March 2019.

[11] J. Selga, J. Coromina, P. Vélez, A. Fernández-Prieto, J. Bonache and F. Martín, "Miniaturised and harmonic-suppressed rat-race couplers based on slow-wave transmission lines," *IET Microwaves, Antennas & Propagation*, vol. 13, no. 9, pp. 1293-1299, 24 7 2019.

[12] F. Martin, "Artificial transmission lines based on periodic structures," in *Artificial Transmission Lines for RF and Microwave Applications*, 1st Ed. Hoboken, NY, USA: John Wiley & Sons, 2015, ch. 2, pp. 47-64

[13] M. A. Antoniades, "Microwave Devices and antennas based on negative-refractive-index transmission-line metamaterials" Ph.D. dissertation, Dept. Electr. and Computer Eng. Toronto Univ., Toronto, Canada, 2009

[14] Qorvo, "General Purpose DPDT Transfer Switch," QPC6222 datasheet, July 2015

[15] Qorvo, "General Purpose Differential 3T Switch 50 MHz to 6000 MHz," RFSW6232 datasheet, June 2015